Progressive massive fibrosis in patients with pneumoconiosis: utility of MRI in differentiating from lung cancer

Yukihiro Ogihara, Kazuto Ashizawa, Hideyuki Hayashi, Takeshi Nagayasu, Tomayoshi Hayashi, Sumihisa Honda, Masataka Uetani

Abstract

Background: It is occasionally difficult to distinguish progressive massive fibrosis (PMF) from lung cancer on computed tomography (CT) in patients with pneumoconiosis.

Purpose: To evaluate the magnetic resonance imaging (MRI) features of PMF and to assess its ability to differentiate PMF from lung cancer.

Material and Methods: Between 2000 and 2014, 40 pulmonary lesions suspected to be lung cancer on the basis of CT in 28 patients with known pneumoconiosis were evaluated. Twenty-four of the 40 lesions were pathologically or clinically diagnosed as PMF. The signal pattern on T2-weighted images (T2WIs), post-contrast enhancement pattern on T1-weighted images (T1WIs), and the pattern of the time intensity curve (TIC) on contrast-enhanced dynamic studies were evaluated. All images were analyzed independently by two chest radiologists.

Results: All 24 PMF lesions showed low signal intensity (SI) on T2WIs (sensitivity, 100%), while 15 of 16 lung cancer lesions showed intermediate or high SI on T2WIs (specificity, 94%) when PMF was regarded as a positive result. Six of 17 PMF lesions showed a homogeneous enhancement pattern (sensitivity, 35%), and four of 9 lung cancer lesions showed an inhomogeneous or a ring-like enhancement pattern (specificity, 44%). Six of 16 PMF lesions showed a gradually increasing enhancement pattern (sensitivity, 38%), and seven of 9 lung cancer lesions showed rapid enhancement pattern (specificity, 78%).

Conclusion: When differentiation between PMF and lung cancer in patients with pneumoconiosis is difficult on CT, an additional MRI study, particularly the T2WI sequence, may help differentiate between the two.

Keywords: Pneumoconiosis, lung cancer, magnetic resonance imaging (MRI), progressive massive fibrosis (PMF), coal worker

Introduction

Pneumoconiosis is caused by the accumulation of inhaled particulate matter which evokes a reaction of the lung tissue (1). Common forms of the disease include silicosis, coal worker's pneumoconiosis, and asbestosis (2). Progressive massive fibrosis (PMF) of the lung is a type of late-stage pneumoconiosis, which is pathologically characterized by conglomeration of silicotic nodules fused by connective tissue (3).

The imaging characteristics of PMF on chest radiography and computed tomography (CT) have been described previously (4-6). However, it is occasionally difficult to distinguish PMF from lung cancer, both clinically as well as on chest radiography and CT. This occurs when a nodule/mass does not exhibit the typical radiological characteristics of PMF, or in the event of development of lung cancer in the backdrop of PMF. Although CT has a high sensitivity for detection of pulmonary nodules and masses, PMF lesions are sometimes difficult to characterize. Therefore, a more invasive diagnostic approach such as biopsy is required to distinguish malignant from benign lesions (7, 8). Typical magnetic resonance imaging (MRI) findings in PMF include low signal intensity (SI) on T2-weighted image (T2WI) (9), and a gradual increase in SI in a dynamic study (10). In one case report, the MRI findings of lung cancer co-existed with those of PMF (11). However, to the best of our knowledge, comparison of MRI findings in PMF and lung cancer has not been reported. According to a previous report, FDG PET may have only a limited role in distinguishing PMF from lung cancer (12). Therefore, MRI examination was performed in addition to CT scan in the cases described above.

The purpose of this study was to evaluate the MRI features of PMF and to

determine the utility of MRI in addition to CT, to differentiate PMF from lung cancer.

Material and Methods

Our institutional review board approved this retrospective study; the requirement for written informed consent of subjects was waived off.

Patients

This retrospective study included 28 patients (all men; mean age 74 years [range, 49-88]) with known pneumoconiosis. Patients were identified on a review of medical records and the radiological database of MRI examinations performed between 2000 and 2014. All 28 patients underwent MRI examinations to differentiate between PMF and lung cancer because of equivocal CT findings. These included pulmonary nodule/mass with irregular or spiculated border in the upper and middle lung zones. Twenty-six patients had a history of smoking (mean, 38.0 pack years). Twenty-seven patients had an employment history that involved dust exposure (coal mining, shipyard work, welding, stone quarry work, and tunnel construction). One patient with no history of occupational dust exposure as per the medical records was diagnosed on the basis of histopathological examination.

Pulmonary lesions were diagnosed pathologically (n = 25) or clinically (n = 15). Pathological specimens included surgical specimens in 18 patients, CT-guided biopsy in 3 patients, transbronchial lung biopsy in 2 patients, and cytological examination in 2 patients. The clinical diagnosis of PMF was based on the CT criteria published by Bergin et al.: an irregular pulmonary nodule/mass, commonly occurring in the upper and middle lung zone and in the areas surrounding the emphysematous lung tissue (13).

Imaging technique

In 28 patients with known pneumoconiosis, 40 pulmonary lesions suspected as lung cancer on CT were imaged with a 1.5-T MRI scanner (Signa Horizon Lx and Signa HDxt, GE Healthcare, Milwaukee, WI, USA) using a torso array coil and a body array coil.

The following MRI sequences were used under free-breathing conditions: 1) T1-weighted image (T1WI): fast spin echo (FSE), repetition time (TR)/echo time (TE) = 500–1100/14 ms; field-of-view = 24–36 cm; matrix size = 160–256 × 256–320; slice thickness = 5−7 mm; slice gap = 1−1.5 mm; 2) T2WI: FSE, TR = 2800–7000 ms; effective TE = 91–104 ms; field-of-view = 24–36 cm; matrix size = 160–256 × 256–320; slice thickness = 5−7 mm; slice gap = 1−1.5 mm; and 3) dynamic study: TR/TE = 5.2–6.1/1.1–1.2 ms, field-of-view = 24–36 cm, matrix size = 160–256 × 256–320; slice thickness = 5−7 mm; and slice gap = 1−1.5 mm. Contrast-enhanced T1WI was obtained for 29 pulmonary lesions in 21 patients, 180 s after an injection of 0.2 mL (0.1 mmol)/kg body weight of gadolinium contrast material at a rate of 3 mL/s. A contrast-enhanced dynamic study was performed for 25 pulmonary lesions in 17 out of the 21 patients, and MR images were obtained 20, 60, 120, and 180 s after contrast injection.

Image interpretation

All images were analyzed independently by two chest radiologists (with 7 and 19 years of experience in image interpretation), who were blinded to the results of pathological findings. In case of any difference in opinion, a consensus was reached

based on discussion. The relative SI of a lesion was compared with that of the skeletal muscle on the same MR image.

The SI pattern of the lesions on T2WI and the post-contrast enhancement pattern of the lesions on T1WI were evaluated. The SI pattern on T2WI was classified into two types: (i) low SI and (ii) intermediate or high SI. With regard to contrast-enhanced studies, in case of enhancing lesions, the enhancement pattern was classified into three types: (i) homogeneous enhancement, (ii) inhomogeneous enhancement, and (iii) ring-like enhancement. With regard to contrast-enhanced dynamic studies, the pattern of the time intensity curve (TIC) was classified into two types: (i) gradually increasing enhancement and (ii) rapid enhancement. Jung et al. classified lesions on the basis of time to peak enhancement after the injection of contrast material; peak enhancement before 180 s after contrast injection was classified as rapid enhancement, while peak enhancement after 180 s of injection was classified as gradual enhancement (10).

According to previous reports, PMF typically shows low SI on T2WI because of fibrosis (9-11), while lung cancer usually shows intermediate to high SI on T2WI. PMF exhibits a homogeneous enhancement pattern as the majority of the lesion consists of fibrosis (9), while lung cancer tends to have an inhomogeneous or a ring-like enhancement pattern (14,15). A gradual increase in enhancement on dynamic contrast-enhanced MR imaging has also been described in PMF (10), while lung cancer shows rapid enhancement as compared to that seen with benign pulmonary nodules (16). Based on these results, a pulmonary lesion was judged to be PMF when it showed low SI on T2WI and a homogeneous enhancement pattern. On the other hand, a pulmonary lesion was judged as lung cancer when it showed intermediate or high SI on T2WI and

an inhomogeneous or a ring-like enhancement pattern. A pulmonary lesion was also judged as PMF when the TIC pattern was gradually increasing enhancement and as lung cancer when the TIC pattern was rapid enhancement. The sensitivity and specificity of MRI was calculated. In addition, we generated the receiver operating characteristic (ROC) curve for the SI pattern of the lesions on T2WI, post-contrast enhancement pattern of the lesions on T1WI, and TIC pattern of the lesions on contrast-enhanced dynamic studies and calculated the area under the ROC curves.

Statistical analysis

Between-group differences with respect to SI pattern of the lesions on T2WI, post-contrast enhancement pattern of the lesions on T1WI, and the pattern of the TIC of the lesions on contrast-enhanced dynamic studies were assessed using Chi-squared test. Inter-observer variations were analyzed by the Kappa coefficient.

Results

Final diagnosis of pulmonary lesions

Twenty-four of the 40 pulmonary lesions were pathologically (n = 9) or clinically (n = 15) diagnosed as PMF. Sixteen pulmonary lesions were diagnosed as lung cancer (7 adenocarcinomas, 6 squamous cell carcinomas, one combined large cell neuroendocrine carcinoma, and 2 cases with cytological diagnosis of carcinoma). There was no evidence of active tuberculosis in any of these patients at the time of this study. The 24 PMF lesions were located in the right upper lobe (RUL) (12 patients), one case each in the right middle lobe (RML) and right lower lobe (RLL); left upper lobe (LUL)

in seven patients; and left lower lobe (LLL) in three patients. The 16 lung cancers were located in the RUL in seven patients, RML in two, RLL in one, LUL in three, and LLL in 3 patients.

MRI findings

The qualitative analysis of the SI pattern on T2WI for 40 pulmonary lesions in 28 patients who underwent MRI study is shown in Table 1. Because all 24 PMF lesions showed low SI on T2WI, the sensitivity was 100% for the diagnosis of PMF on the basis of SI pattern on T2WI (Fig. 1). Fifteen of 16 lung cancer lesions showed intermediate or high SI on T2WI; the specificity was 94% (Fig. 2). The remaining one lesion, which was lung cancer, was judged as false positive (PMF) on the basis of an area of predominantly low SI on T2WI. In this case, lung cancer co-existed with PMF that occupied the majority of the lesion pathologically (Fig. 3). A statistically significant difference was found between lesions showing low SI and those showing intermediate or high SI on T2WI ($p < 0.001$). The area under the ROC curve of SI pattern on T2WI was 0.969.

The qualitative analysis of the enhancement pattern on T1WI for 29 pulmonary lesions in 21 patients who underwent contrast-enhanced MRI study is shown in Table 2. Two PMF lesions and one lung cancer had no enhancement. As six of the 17 PMF lesions showed homogeneous enhancement, the diagnosis of PMF on the basis of the post-contrast enhancement pattern on T1WI showed a sensitivity of 35% (Fig. 1). Four of nine lung cancer lesions showed an inhomogeneous or a ring-like enhancement pattern, which corresponded with a specificity of 44%. No statistically significant difference was observed between the lesions showing homogeneous enhancement

pattern and those showing inhomogeneous or a ring-like enhancement pattern (p = 0.320). The area under the ROC curve of post-contrast enhancement pattern on T1WI was 0.601.

Table 3 shows the qualitative analysis of the SI pattern on T2WI, post-contrast enhancement pattern on T1WI, and TIC pattern of 25 pulmonary lesions in the 17 patients who underwent contrast-enhancement dynamic study. The sensitivity, specificity, and area under the ROC curve for the SI pattern on T2WI were 100%, 100%, and 1.0, respectively. A statistically significant difference was found between lesions showing low SI and those showing intermediate or high SI on T2WI ($p < 0.001$). The sensitivity, specificity, and area under the ROC curve for the enhancement pattern were 38%, 44%, and 0.59, respectively. No statistically significant difference was observed between the lesions showing homogeneous enhancement pattern and those showing inhomogeneous or a ring-like enhancement pattern (p = 0.383). In terms of the TIC pattern, six of the 16 PMF lesions showed a gradually increasing enhancement pattern, indicating a sensitivity of 38% (Fig. 4). Seven of the 9 lung cancer lesions showed rapid enhancement, with a corresponding specificity of 78%. No statistically significant difference was observed between the lesions showing gradual increase in enhancement and those showing rapid enhancement (p = 0.432). The area under the ROC curve of TIC pattern was 0.576.

Inter-observer agreement

The Kappa coefficient for inter-observer agreement in assessment of the signal pattern on T2WI was r = 0.9474, which indicated a very good inter-observer agreement; the corresponding Kappa coefficient for post-contrast enhancement pattern T1WI was r

= 0.7665, which indicated a good agreement.

Discussion

The typical CT features of PMF are well-documented; these include, irregular nodule/mass with calcification, commonly occurring in the upper and middle lung zones and in areas surrounding the emphysematous lung tissue (13). PMF can increase slowly in size in general, and move towards the hilar region (6,13). However, a nodule/mass that does not exhibit typical radiographic characteristics of PMF, is liable to be misdiagnosed as lung cancer on the basis of CT findings. Although a nodule/mass in the lower lung zone of a patient with pneumoconiosis is not likely to be PMF, a similar lesion in the upper and middle lung zones may sometimes be difficult to distinguish between PMF and lung cancer on CT. We predicted that the SI pattern on T2WI is useful in distinguishing PMF from lung cancer because PMF lesions show low SI on T2WI, owing to the fibrosis (9,11), while lung cancer usually shows high or intermediate SI on T2WI. Therefore, since 2000, we have performed MRI examination in addition to CT in cases of pneumoconiosis where differentiation between PMF and lung cancer is not straightforward on the basis of CT findings alone.

We found T2WI as the most useful sequence for distinguishing PMF from lung cancer. All PMF lesions showed low SI on T2WI. Low SI on T2WI correlated with the fibrotic tissue. One false positive lesion (positive predictive value, 96%) showing low SI on T2WI was due to co-existence of silicotic nodules and lung cancer, and predominantly composed of fibrotic tissue with silicotic nodules (Fig. 3). PMF associated with inflammation may show high SI on T2WI, resulting in a false negative, although no such cases were observed in this study.

In our study, post-contrast enhancement pattern on T1WI had low sensitivity and specificity for distinguishing PMF from lung cancer. The diagnostic performance of enhancement pattern was inferior to that of T2WI. Therefore, it is difficult to distinguish PMF from lung cancer on the basis of enhancement pattern on T1WI.

Jung et al. reported a marked, gradual increase in SI in a dynamic study of PMF (10). On the other hand, Fujimoto et al. reported that lung cancers showed more rapid enhancement as compared to that shown by benign pulmonary nodules on dynamic MRI (16,17). In our study, only six of 16 PMF lesions (38%) showed a gradually increasing enhancement. The low sensitivity observed differs from that reported by Jung et al. In this study, MRI examinations were not performed in all patients with PMF. Therefore, patient selection bias may have influenced the observed differences in enhancement pattern observed in our dynamic study.

Our study had several limitations. First, all patients with pneumoconiosis did not undergo MRI studies because MRI studies were not performed in typical cases of PMF. However, we believe that MRI studies should be performed only in selected cases based on a cost-benefit evaluation. Secondly, the number of patients in this study was relatively small. Patients with pneumoconiosis complicated by lung cancer are not common, and these are likely to decrease with a decrease in number of new pneumoconiosis patients in the future. To accumulate further cases, we will prospectively perform additional MRI studies in patients where differentiation between PMF and lung cancer is difficult on CT. Thirdly, different MRI machines and protocols were used because this was a long-term study. However, these variations did not affect the main results of this study.

In conclusion, when differentiation between PMF and lung cancer is difficult

on CT in patients with pneumoconiosis, an additional MRI study, particularly T2WI, may help differentiate between the two, as PMF lesions show low signal intensity, while lung cancer lesions show intermediate or high SI.

Acknowledgments

We are grateful to Kazuhiro Tabata, MD; Junya Fukuoka, MD; Naoya Yamasaki, MD; and Keitaro Matsumoto, MD for their helpful comments.

References

1. Fourth International Pneumoconiosis Conference, Report of the Working Party on the Definition of Pneumoconiosis, International Labour Organization, Geneva, Switzerland, 1971.
2. Chong S, Lee KS, Chung MJ, et al. Pneumoconiosis: Comparison of imaging and pathologic findings. Radiographics 2006; 26: 59-77.
3. Gibbs AR. Occupational lung disease. In: Hazleton PA, ed. Spencer's pathology of the lung. 5th ed. New York: McGraw Hill, 1996; pp.461-504.
4. Williams JL, Moller GA. Solitary mass in the lungs of coal miners. Am J Roentgenol Radium Ther Nucl Med 1973; 117: 765-770.
5. Soutar CA, Collins HP. Classification of progressive massive fibrosis of coalminers by type of radiographic appearance. Br J Indust Med 1984; 41: 334-339.
6. Remy-Jardin M, Degreef JM, Beuscart R, et al. Coal worker's pneumoconiosis: CT assessment in exposed workers and correlation with radiographic findings. Radiology 1990; 177: 363-371.
7. Dholakia S, Rappaport DC. The solitary pulmonary nodule. Is it malignant or benign? Postgrad Med 1996; 99: 246-250.
8. Viggiano RW, Swensen SJ, Rosenow EC 3rd. Evaluation and management of solitary and multiple pulmonary nodules. Clin Chest Med 1992; 13: 83-95.
9. Matsumoto S, Mori H, Miyake H, et al. MRI signal characteristics of progressive massive fibrosis in silicosis. Clin Radiol 1998; 53: 510-514.
10. Jung JI, Park SH, Lee JM, et al. MR characteristics of progressive massive fibrosis. J Thorac Imaging 2000; 15: 144-150.
11. Matsumoto S, Miyake H, Takaki H, et al. Diagnosis of lung cancer in a patient with

pneumoconiosis and progressive massive fibrosis using MRI. Eur Radiol 1998; 8: 615-617.

12. Chung SY, Lee JH, Kim TH, et al. ^{18}F-FDG PET imaging of progressive massive fibrosis. Ann Nucl Med 2010; 24: 21-27.
13. Bergin CJ, Müller NL, Vedal S, et al. CT in silicosis: correlation with plain films and pulmonary function tests. Am J Roentgenol 1986; 146: 477-483.
14. Tozaki M, Suzuki M, Takeda H, et al. Three-dimensional dynamic MR imaging with a volumetric interpolated breath-hold examination for solitary pulmonary lesions: correlation of contrast enhancement pattern with pathological features. Nihon Igaku Housyasen Gakkai Zasshi 2004; 64: 13-21.
15. Donmez FY, Yekeler E, Saeidi V, et al. Dynamic contrast enhancement patterns of solitary pulmonary nodules on 3D gradient-recalled echo MRI. Am J Roentgenol 2007; 189: 1380-1386.
16. Fujimoto K. Usefulness of contrast-enhanced magnetic resonance imaging for evaluating solitary pulmonary nodules. Cancer Imaging 2008; 8: 34-44.
17. Kohno R, Fujimoto K, Terasaki H, et al. Dynamic MRI of solitary pulmonary nodules: comparison of enhancement patterns of malignant and benign small peripheral lung lesions. Am J Roentgenol 2007; 188: 26-36.

Table 1. Qualitative analysis of the SI pattern on T2WI for 40 lesions in 28 patients who underwent MRI study

	PMF	Lung cancer	Total
SI pattern of the lesion			
Low	24	1	25
Intermediate or high	0	15	15
Total	24	16	40

A statistically significant difference was found between lesions showing low SI and those showing intermediate or high SI on T2WI ($p < 0.001$).

SI, signal intensity; T2WI, T2-weighted image; MRI, magnetic resonance imaging; PMF, progressive massive fibrosis;

Table 2. Qualitative analysis of the enhancement pattern on T1WI for 29 lesions in 21 patients who underwent contrast-enhanced MRI study

	PMF	Lung cancer	Total
Non-enhancing lesion	2	1	3
Enhancing lesion	17	9	26
Homogeneous	6	5	11
Inhomogeneous or ring-like	11	4	15
Total	19	10	29

No statistically significant difference was observed between the lesions showing homogeneous enhancement pattern and those showing inhomogeneous or a ring-like enhancement pattern ($p = 0.320$).

MRI, magnetic resonance imaging; PMF, progressive massive fibrosis

Table 3. Qualitative analysis of the SI pattern on T2WI, post-contrast enhancement pattern on T1W1, and TIC pattern for 25 lesions in 17 patients who underwent contrast-enhanced dynamic MRI study

	PMF	Lung cancer	Total
SI pattern of the lesion on T2WI			
Low	16	0	16
Intermediate or high	0	9	9
Enhancement pattern of the lesion			
Homogeneous	6	5	11
Inhomogeneous or ring-like	10	4	14
TIC pattern of the lesion			
Gradually increasing enhancement	6	2	8
Rapid enhancement	10	7	17
Total	16	9	25

A statistically significant difference was found on T2WI ($p < 0.001$). However, no statistically significant difference was found between the enhancement pattern ($p = 0.383$) and TIC pattern ($p = 0.432$).

SI, signal intensity; T2WI, T2-weighted image; TIC, time intensity curve; MRI, magnetic resonance imaging; PMF, progressive massive fibrosis

Figure legends

Fig. 1. A 78-year-old male with PMF confirmed on histopathological examination of surgical specimen

(a) Thin-section CT image showing a well-defined nodule with pleural indentation in the right upper lobe. Multiple small nodules indicative of pneumoconiosis are also seen in the surrounding lung tissue.

(b) The nodule has an inhomogeneous enhancement pattern on contrast-enhanced CT. It was difficult to differentiate PMF from lung cancer on the basis of CT findings.

(c, d) The nodule showed very low SI on T2WI (C) and an inhomogeneous enhancement pattern on contrast-enhanced T1WI of MRI (D).

(e) Histopathological image showing nodular fibrosis with acellular collagenous proliferation (*). Multinodular changes with anthracotic pigments are seen at the periphery of these fibrous nodules (Arrows).

Fig. 2. A 71-year-old male with histopathological diagnosis of lung cancer

(a) A thin-section CT image showing a well-defined mass in the right upper lobe. Multiple small nodules indicative of pneumoconiosis are also seen in the surrounding lung.

(b, c) The mass showed slightly high SI on T2WI (B) and an inhomogeneous enhancement pattern on contrast-enhanced T1WI of MRI (C).

(d, e) TIC showed a rapid enhancement pattern.

(f) Histopathological image showing adenocarcinoma. The tumor consisted of papillary non-mucinous carcinoma cell growth with high cellularity.

Fig. 3. A 70-year-old male with PMF complicated by histopathologically confirmed lung cancer

(a) Thin-section CT image showing a well-defined nodule with pleural indentation in the right upper lobe. Multiple small ground-glass nodules indicating pneumoconiosis are also seen in the surrounding lung.

(b) The majority of the lesion showed a very low SI area (arrow) on T2WI, but the dorsal part of the lesion had high SI (arrowhead). We judged the nodule to be PMF on the basis of the predominantly low SI area on T2WI.

(c) Histopathological image showed upper half of fibrous tissue and lower half of adenocarcinoma. Fibrous area (*) consisted of dense collagen bundles and brown anthracotic pigment deposition. Lower half showed adenocarcinoma cells proliferating along the alveolar structure, showing lepidic and papillary growth. There were hemosiderin-laden cells in the air space, which indicates tumor hemorrhage. Upper half of fibrous tissue corresponded to very low SI on T2WI, and lower half of adenocarcinoma corresponded to high SI on T2WI.

Fig. 4. A 69-year-old male with PMF diagnosed clinically.

(a) Thin-section CT image showing ill-defined nodules with spiculation in the right upper lobe;

(b, c) The nodules showed very low SI on T2WI (B) and a homogeneous enhancement pattern on contrast-enhanced T1WI of MRI (C).

(d, e) TIC showed gradually increasing enhancement.

Figure 1

(a)

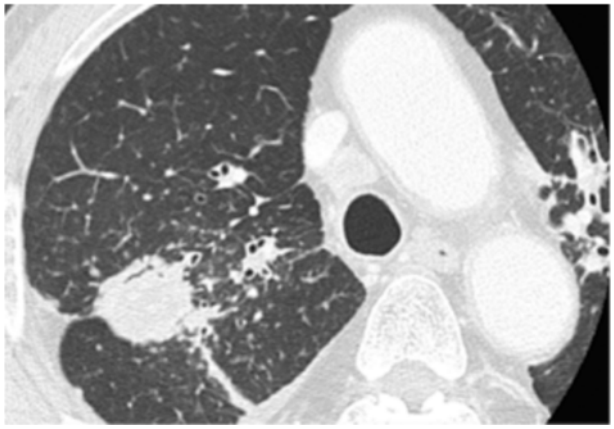

(b)

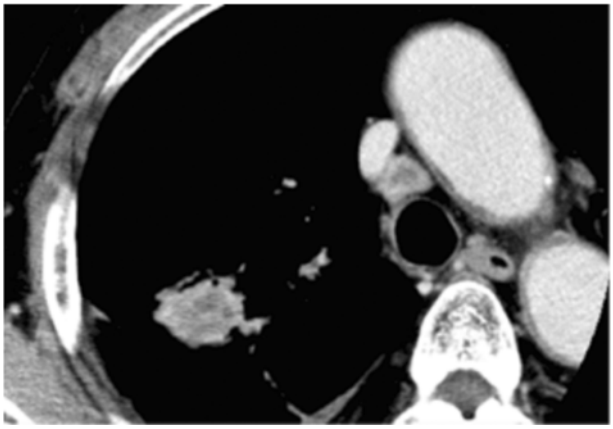

(c)

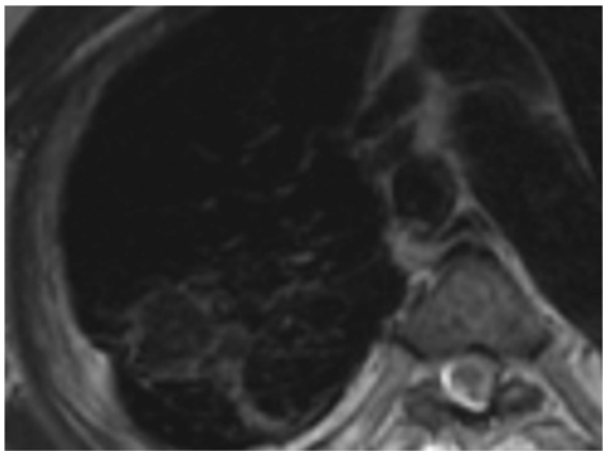

(d)

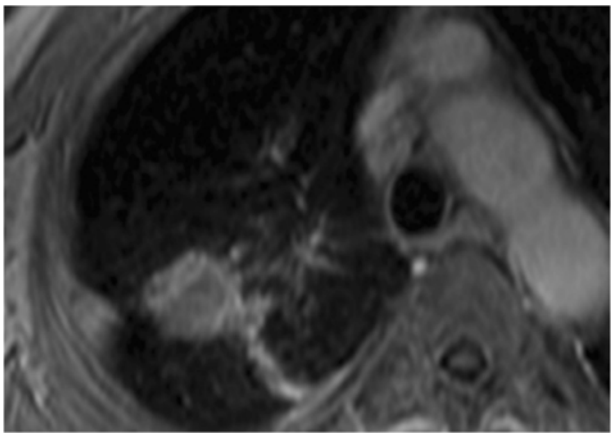

(e)

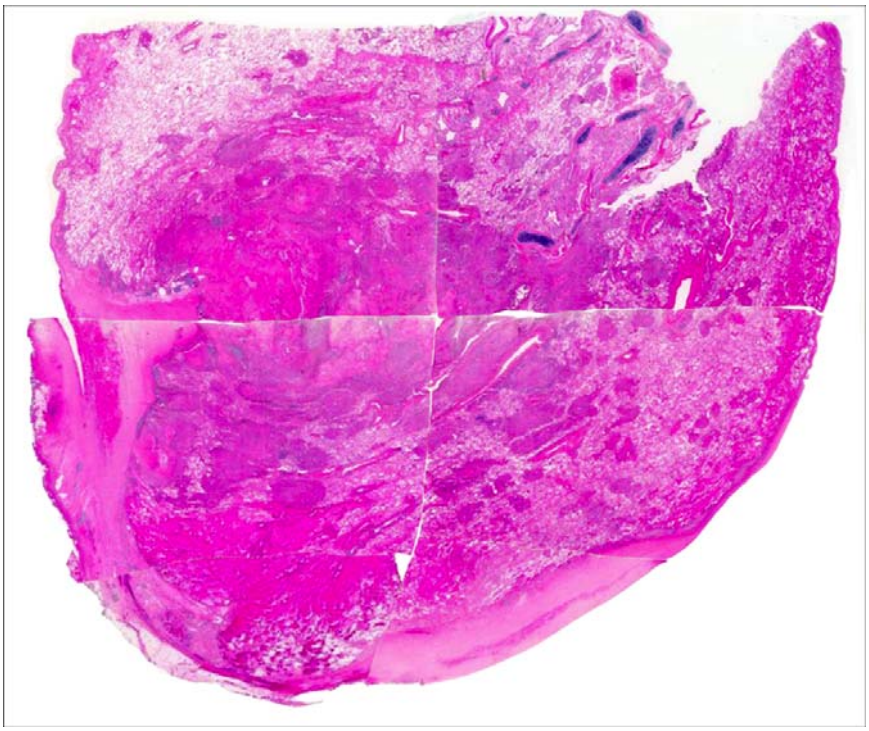

Figure 2

(a)

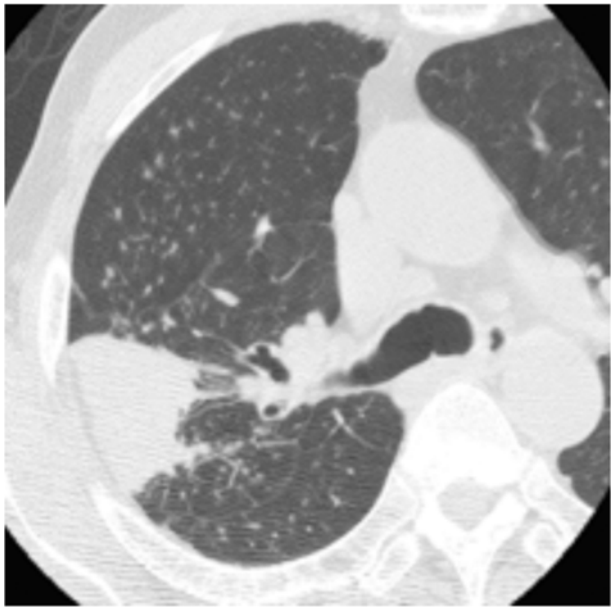

(b)

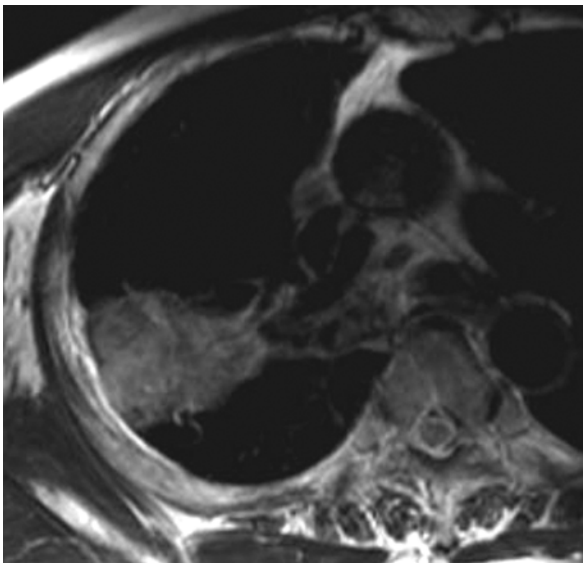

(c)

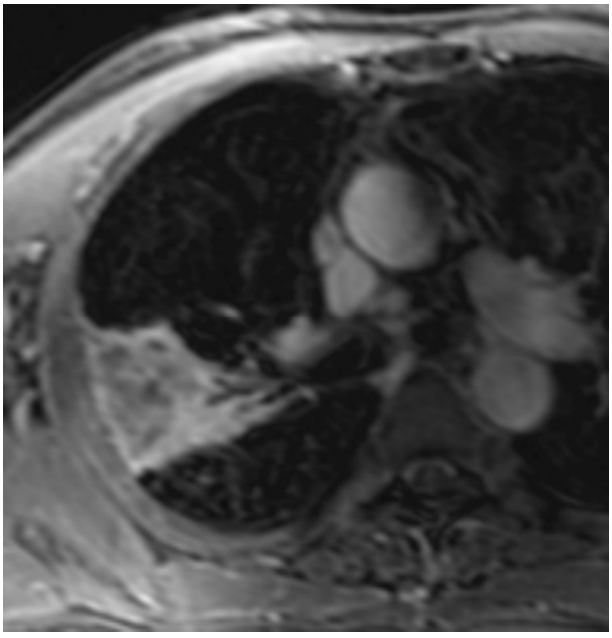

(d)

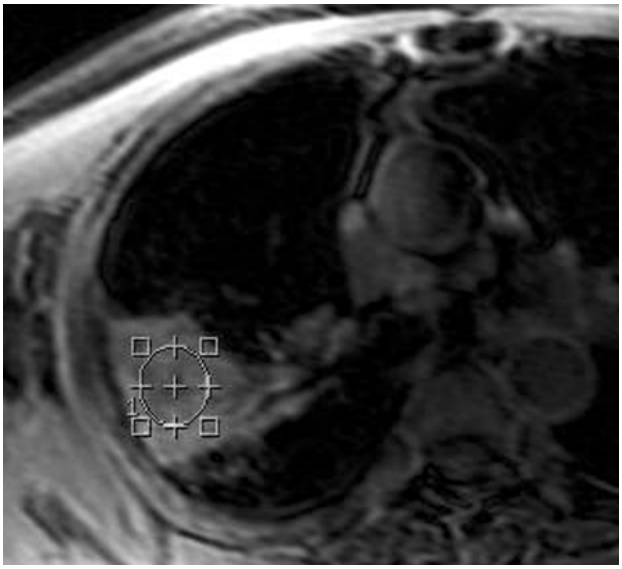

(e)

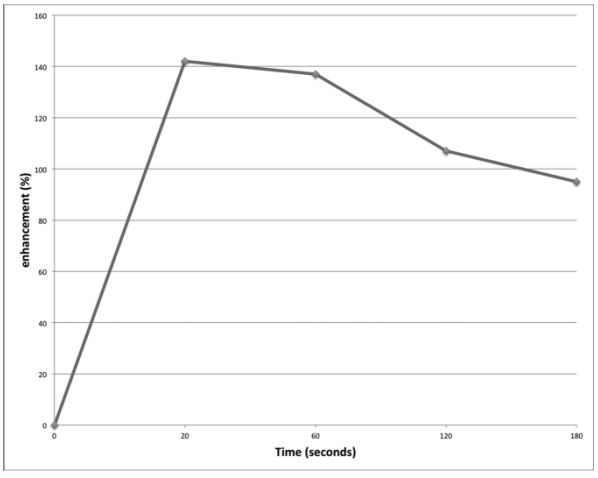

(f)

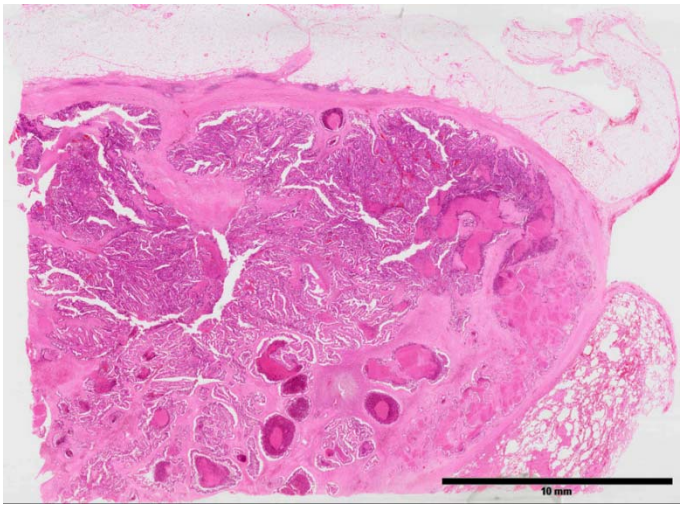

Figure 3

(a)

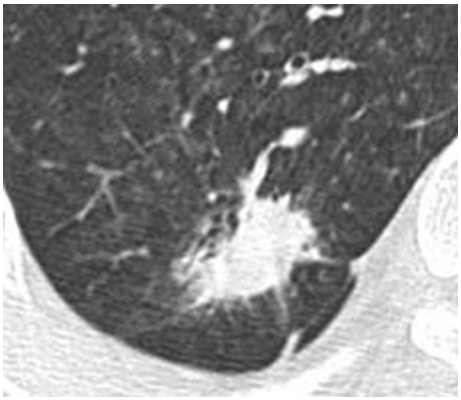

(b)

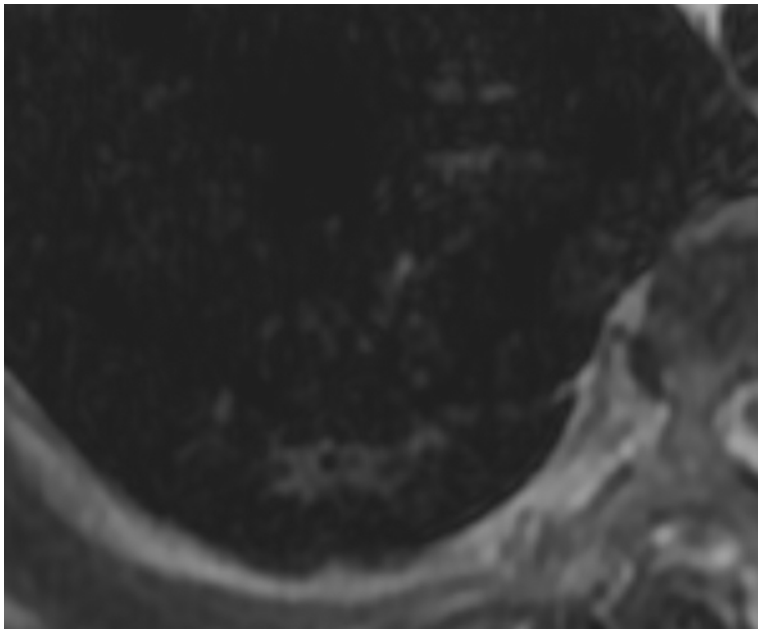

(c)

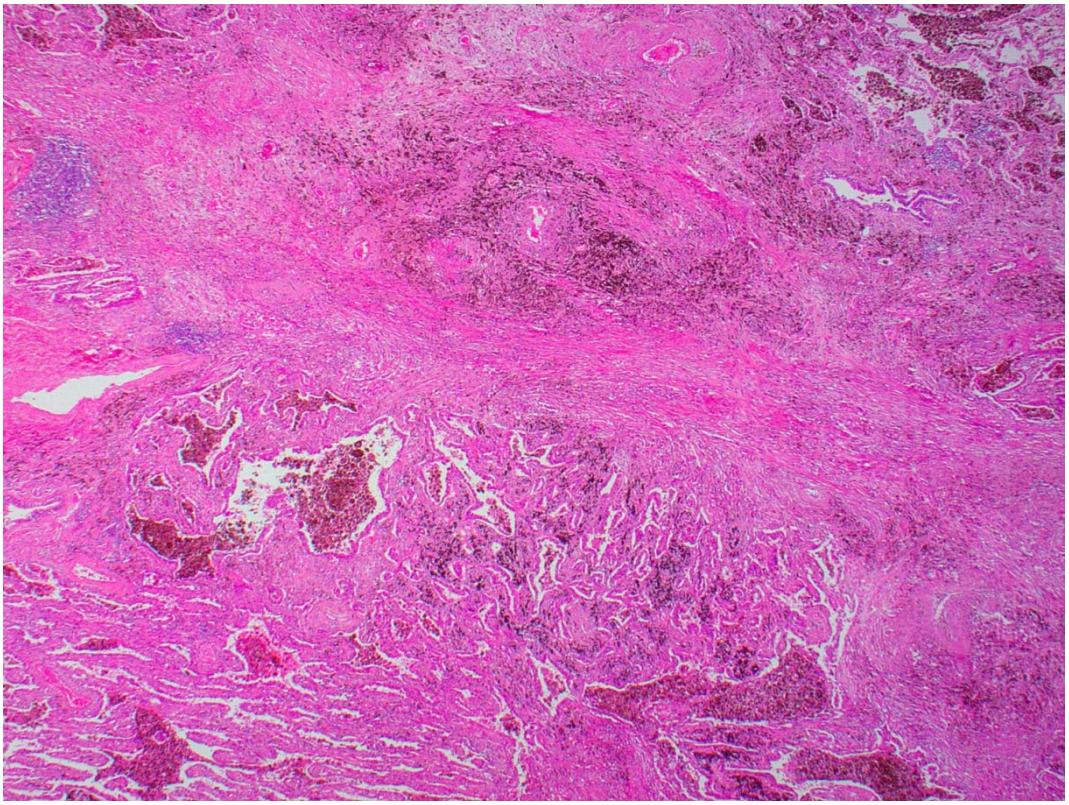

Figure 4

(a)

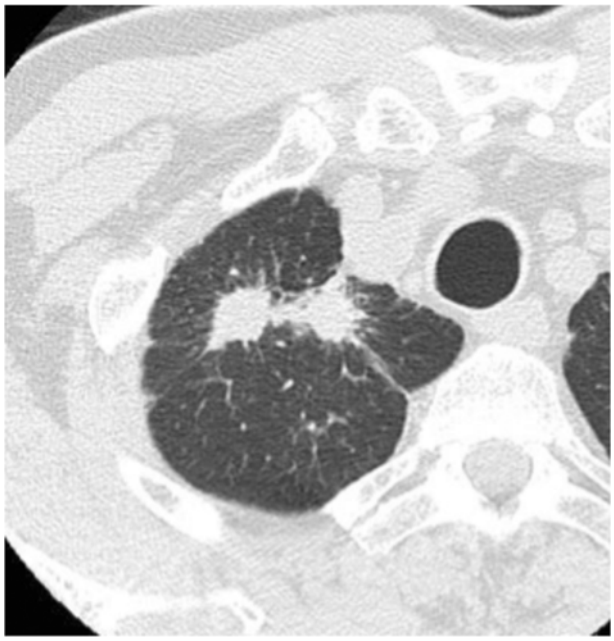

(b)

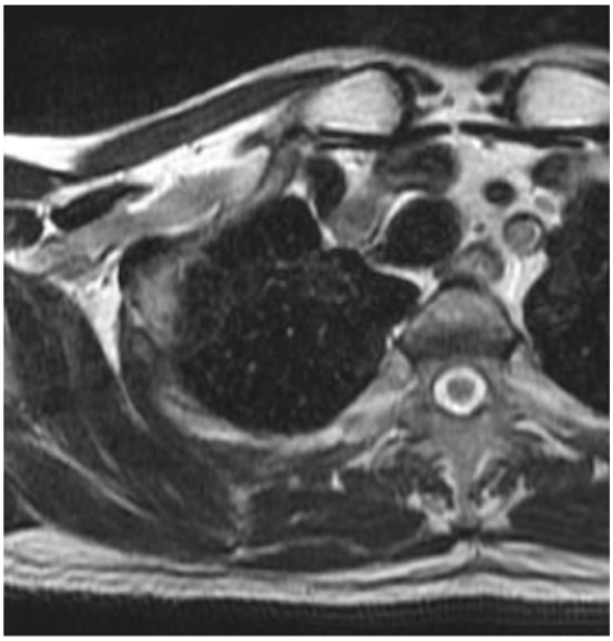

(c)

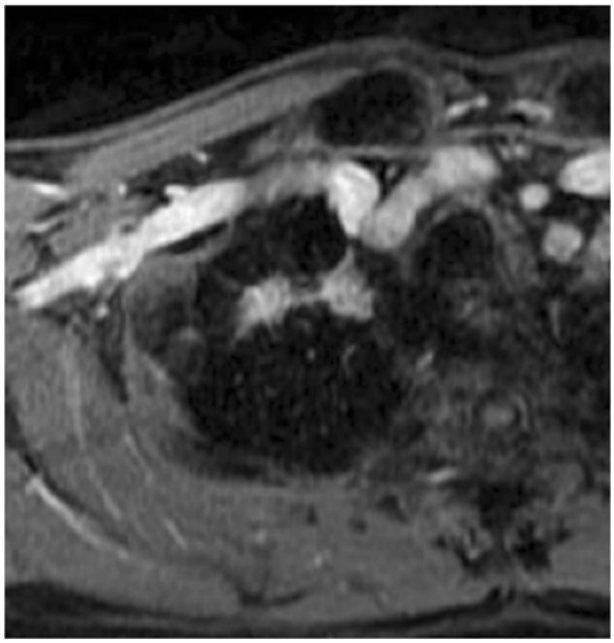

(d)

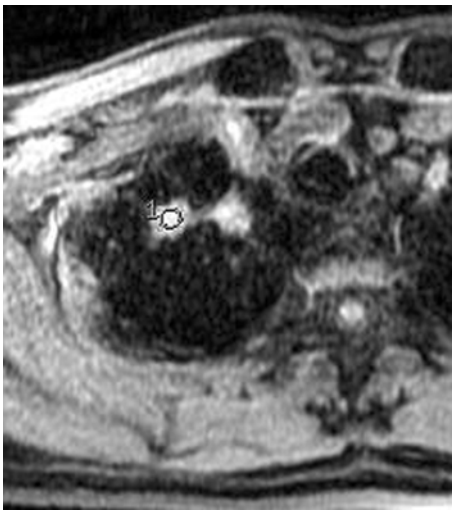

(e)